COMSOL CONFERENCE 2020 EUROPE

Diffraction Efficiency of Gratings with Sinusoidal Profile

P. Janicek[1,2,*], V. Stepankova[3], M. Kurka[4], K. Palka[4,2], A. Ventura[5], J. G. Hayashi[5]
1. Institute of Applied Physics and Mathematics, Faculty of Chemical Technology, University of Pardubice, Pardubice, 53210, Czech Republic
2. Center of Materials and Nanotechnologies, Faculty of Chemical Technology, University of Pardubice, Pardubice, 53210, Czech Republic
3. Department of Graphic Arts and Photophysics, Faculty of Chemical Technology, University of Pardubice, Pardubice, 53210, Czech Republic
4. Department of General and Inorganic Chemistry, Faculty of Chemical Technology, University of Pardubice, Pardubice, 53210, Czech Republic
5. Optoelectronics Research Centre, University of Southampton, Southampton, SO17 1BJ, UK
* e-mail: petr.janicek@upce.cz

Introduction

One of the diffraction gratings fabrication process is hot-embossing. In this process, the master grating is pressed into a glass layer pre-heated above its glass transition temperature. Our aim is to fabricate gratings with sinusoidal profile with defined depth. Different depth of diffraction grating can be obtained by using different pressure, time or temperature in the pressing process. We would like to find out whether the measurement of diffraction efficiency (DE) of the grating can be used to determine the grating thickness. If this measurement is possible during the forming process (in-situ), it would be a great benefit for the diffraction grating fabrication as by fine-tuning the fabrication parameters (as temperature, pressure time, …) to obtain target DE during hot-embossing would lead to fabrication of the diffraction grating with required depth. As the first step, we would like to access, theoretically and experimentally, the DE of 16 diffraction gratings fabricated with different depths ex-situ.

The diffraction efficiency identifies the energy of radiation, which is transferred and divided into individual diffraction orders. Relative diffraction efficiency determines the ratio of the intensity of electromagnetic radiation in a given diffraction order I_m to the intensity of incident radiation on the material I_0. For theoretical calculation of the diffraction efficiency (with assumption that wavelength of the light λ is greater than the depth of the diffraction grating h) equation 1 can be used [1]. This equation is valid for sinusoidal profile of the diffraction grating and involves the solution of the Bessel functions:

$$\eta_m = J_m^2 \left\{ \frac{\pi h}{\lambda} (cos\alpha + cos\alpha_m) \right\} \quad (1)$$

where η_m is diffraction efficiency of m-th diffraction order, J_m is the Bessel function of the first kind and m-th order, h depth of the grating, λ wavelength of the incident light, α_m angle of the m-th diffraction order and α angle of incidence (see fig. 1). Equation 1 is derived for an ideally reflecting material and should be corrected by multiplying by the reflectivity of the material. Moreover eq. 1 does not involve orientation of the incident wave.

The distribution of energy that is diffracted into individual diffraction orders at a given wavelength depends on many parameters (e.g. polarization of incident light, angle of incidence, refractive index of the material from which the grating is made and the period of the grating). As early as 1874, Lord Rayleight noted that the adjustment of the grating profile could alter the distribution of the energy into the diffraction orders [2].

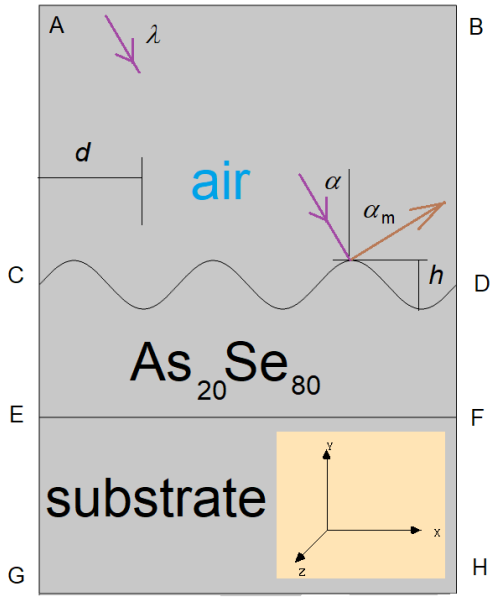

Figure 1. Diffraction grating simulated geometry.

Theory / Experimental Set-up

Our gratings were fabricated deposing a layer of amorphous $As_{20}Se_{80}$ (thickness t = 970 nm) onto soda-lime glass substrates by thermal evaporation. Sixteen gratings with different depths h (from 10 to 150 nm) were produced by hot-embossing at temperature range 100 – 140 °C [3] using a master made of polydimethylsiloxane with a sinusoidal profile and period d = 860 nm.

The optical constants (spectral dependence of the refractive index n and the extinction coefficient k) of the soda-lime glass substrate and the $As_{20}Se_{80}$ layer were determined in the spectral range 300-1000 nm by spectroscopic ellipsometry using a VASE ellipsometer (J. A. Woollam Co.) and three angles of incidence 55, 65 and 75° (see fig. 2). The reflectivity used to

correct equation 1 can be calculated from optical constants and / or measured by the same instrument. The diffraction profile and the depth of the prepared gratings were measured by atomic force microscopy (Solver NEXT, NT-MDT) in semicontact mode (see fig. 3 as an example).

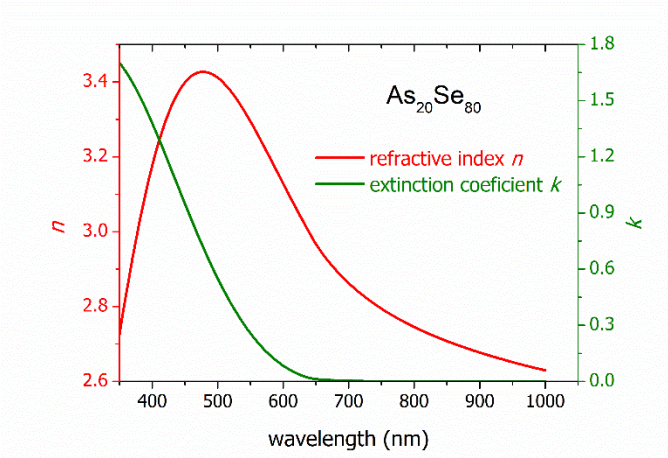

Figure 2. Spectral dependence of the refractive index n and the extinction coefficient k of the $As_{20}Se_{80}$ layer determined using spectroscopic ellipsometry.

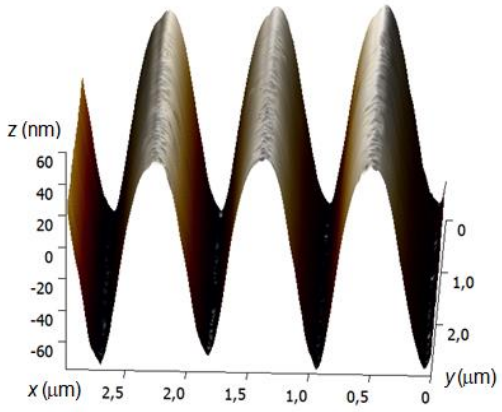

Figure 3. Example of diffraction grating profile measured using atomic force microscopy.

In order to assess the diffraction efficiency experimentally, a custom-made setup consisting of a LED diode source, a photodiode detector and a rotating sample stage was used (see fig. 4). Our stage allows the change of the angle of incidence and the angle of detection, which can be adjusted to measure different diffraction orders (STANDA in Lithuania). The intensity of the incident light, together with the position and the intensity of the m-th diffraction order maxima (for m = 0, 1 and -1) were measured for each grating using a red (λ = 635 nm) and a green (λ = 532 nm) diode (Thorlabs Inc., USA). In our measurement, the electric current produced by the photodiode was used instead of the intensity of the light with assumption of linearity between them.

The position of the m-th diffraction maxima in the reflection (i.e. diffraction angle α_m) is given by the grating equation

$$m \cdot \lambda = d \cdot n_{air} \cdot (sin\alpha_m - sin\alpha) \quad (2)$$

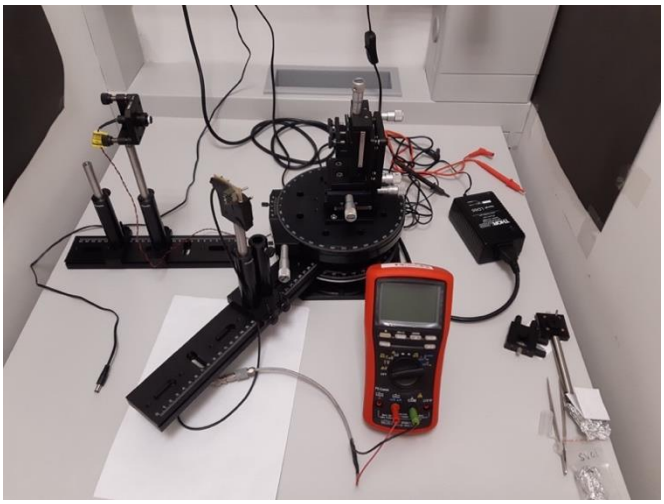

Figure 4. Custom-made equipment employed in our diffraction efficiency measurement.

Governing Equations / Numerical Model / Simulation / Methods / Use of Simulation Apps

Table 1: Material properties used as an input for the model

Air	n = 1 (wavelength independent)
Glass	$As_{20}Se_{80}$
n (λ = 532 nm) = 1.5168 n (λ = 635 nm) = 1.5132	n (λ = 532 nm) = 3.3456 n (λ = 635 nm) = 3.0129
k (λ = 532 nm) = = k (λ = 635 nm) = 0	k (λ = 532 nm) = 0.3479 k (λ = 635 nm) = 0.0235

Table 2: Other input parameters used in the model

Grating period	d = 860 nm
$As_{20}Se_{80}$ thickness	$\lvert CE \rvert$ = 970 nm
Wavelength	λ = 532 nm (green) and 635 nm (red)
Angle of incidence	α = 0, 5 and 10 deg
Grating depth	h from 0 to 150 nm with 10 nm step

To set up the numerical modelling in COMSOL 5.5, a procedure similar to the Plasmonic wire grating model application using Wave optics module was taken as the guide.
The model geometry consists of one unit cell of length d with three domains representing the air above the grating, the material of the grating and the glass substrate. The thickness of glass substrate and air was chosen to $3 \cdot \lvert CE \rvert$.
To simulate the electric field spatial distribution, we used the electromagnetic waves frequency domain Physics. Similarly to the Plasmonic wire grating model application, in-plane and out-of-plane components of the electric field vector were studied independently. The aim of our calculation is to obtain the

electric field vector $\boldsymbol{E}$ for all (x, y, z) by solving the time independent wave equation.

$$\nabla \times \left(\mu_r^{-1} \nabla \times \vec{E}\right) - k_0^2 n^2 \vec{E} = \vec{0} \quad (3)$$

where $\tilde{n}$ and μ_r are the material dependent optical properties (the complex refractive index $\tilde{n}$ consists of a real part n and an imaginary part k), and the magnetic properties (relative permeability μ_r = 1), respectively. The k_0 is wave number of free space:

$$k_0 = \omega\sqrt{\varepsilon_0 \mu_0} = \frac{\omega}{c_0} \quad (4)$$

where c_0 is the speed of light in vacuum and $\omega = 2\pi f = \frac{2\pi c}{\lambda}$ is defined by wavelength λ.

Used boundary conditions:
[AC], [CE], [EG], [BD], [DF], [FH] periodic boundary conditions

$$\overrightarrow{E_{tangential}}(\overrightarrow{r_B}) = \overrightarrow{E_{tangential}}(\overrightarrow{r_A}) \cdot exp\left(-i\vec{k} \cdot (\overrightarrow{r_B} - \overrightarrow{r_A})\right) \quad (5)$$

[AB] incident periodic electromagnetic wave

$$\vec{E}(x, y, z) = A \cdot exp(-i\vec{k} \cdot \vec{r}) \quad (6)$$

Out-of-plane $\boldsymbol{E}$ = (0, 0, 1) and in-plane $\boldsymbol{H}$ = (0, 0, 1) incident wave calculated independently.
Automatic diffraction order reflectance calculation used.
[GH] output periodic electromagnetic wave. Automatic diffraction order transmittance calculation used.

Parameter sweep study used to access different angle of incidence and grating depths.

Experimental Results / Simulation Results / Discussion

1) Green LED diode

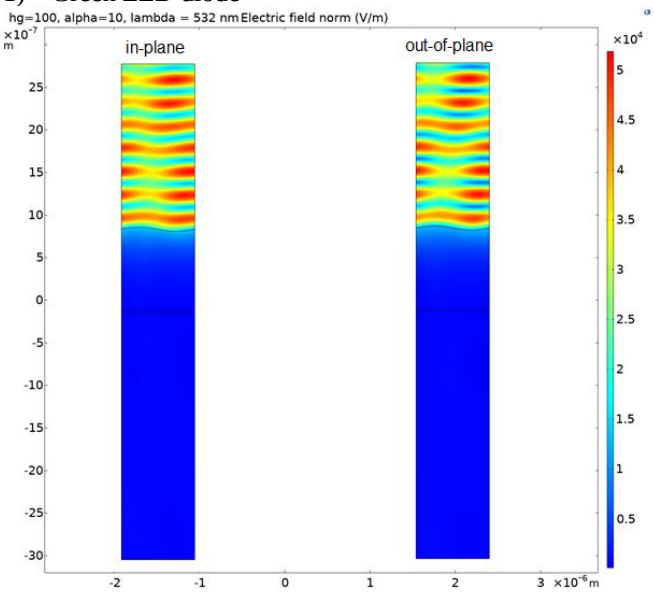

Figure 5. Spatial distribution of the electric field (electric field norm) for a green LED, h = 100 nm and α = 10 deg.

One example of the calculated electric field spatial distribution for the in-plane (left side) and out-of-plane (right side) incident wave is depicted at fig. 5. Due to the high extinction coefficient of the $As_{20}Se_{80}$ layer, the electric field is practically zero in substrate (almost zero transmittance). Figure 6 shows the dependence of the 1st, minus 1st and zero order reflectance as a function of the grating depth. Especially, dependence of the first diffraction order intensity on the grating depth can be used for the experimental grating depth measurement.

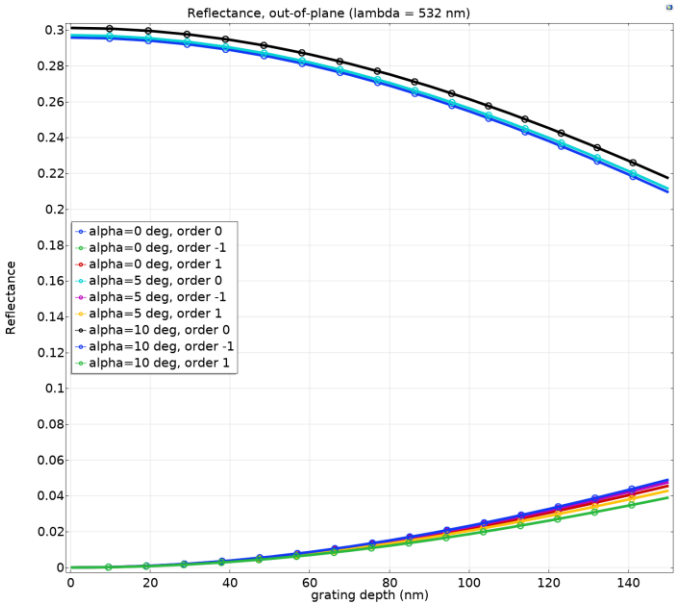

Figure 6. Dependence of the different diffraction order reflectance on grating depth for three angles of incidence.

The comparison of the DE experimentally measured for our 16 fabricated diffraction gratings to the calculation using the Bessel functions (eq. 1) and the reflectance modeled using COMSOL is depicted in figs. 7-9. Figure 7 shows the dependence of the 1st diffraction order reflectance on the grating depth. The results obtained using the simulation in COMSOL are slightly lower in comparison to experimental results as well as the analytical calculation using the Bessel functions.

Similar result can be found for the minus 1st diffraction order reflectance (see fig. 8 as an example).

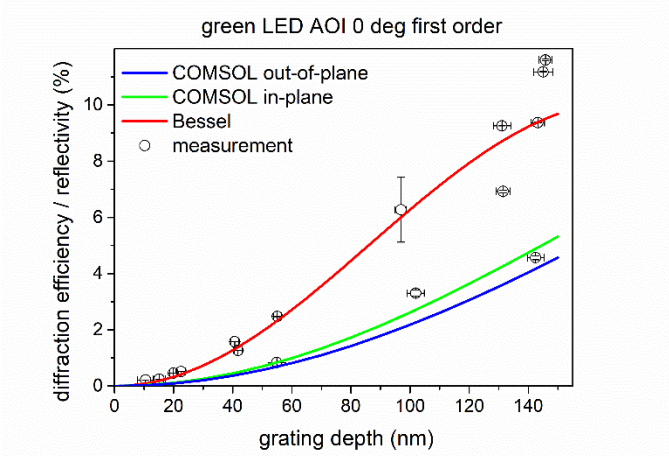

Figure 7. Comparison of the dependence of the 1st diffraction order reflectance / diffraction efficiency on the grating depth for green LED and $\alpha = 0$ deg obtained experimentally and theoretically.

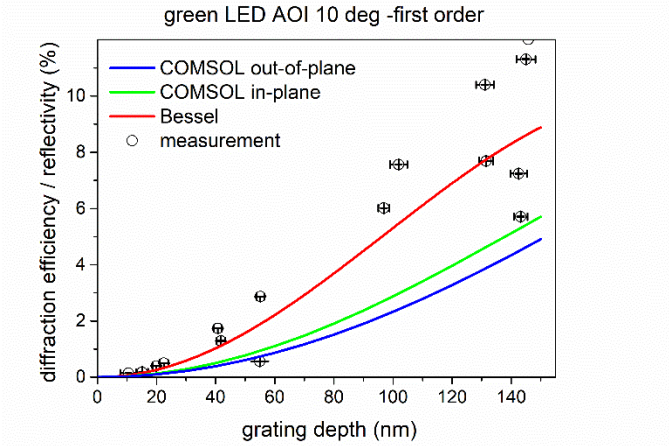

Figure 8. Comparison of the dependence of the minus 1st diffraction order reflectance / diffraction efficiency on the grating depth for green LED and $\alpha = 10$ deg obtained experimentally and theoretically.

In the case of zero diffraction order, the behavior is the opposite. The decrease of the zero diffraction order reflectance calculated using COMSOL as a function of the grating depth is slightly less pronounced than the analytical calculation using the Bessel function and the experimental results (see fig. 9).

Results obtained by "polarization independent" analytical formula are in case of green LED closer to the experimental data.

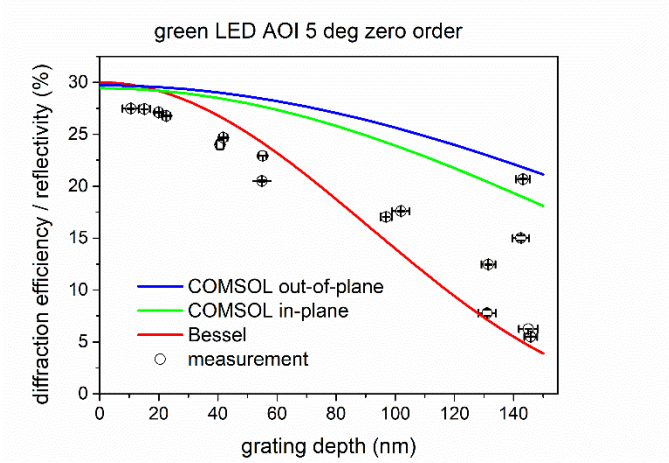

Figure 9. Comparison of the dependence of the zero diffraction order reflectance / diffraction efficiency on the grating depth for green LED and $\alpha = 5$ deg obtained experimentally and theoretically.

2) Red LED diode

Changing the input parameters in the model, the same calculation was performed for the red diode. Due to the lower extinction coefficient of $As_{20}Se_{80}$ layer in such wavelength (by one order of magnitude), the electric field propagates through the layer to the soda-lime glass substrate, as it can be seen from the electric field spatial distribution calculation (see fig. 10).

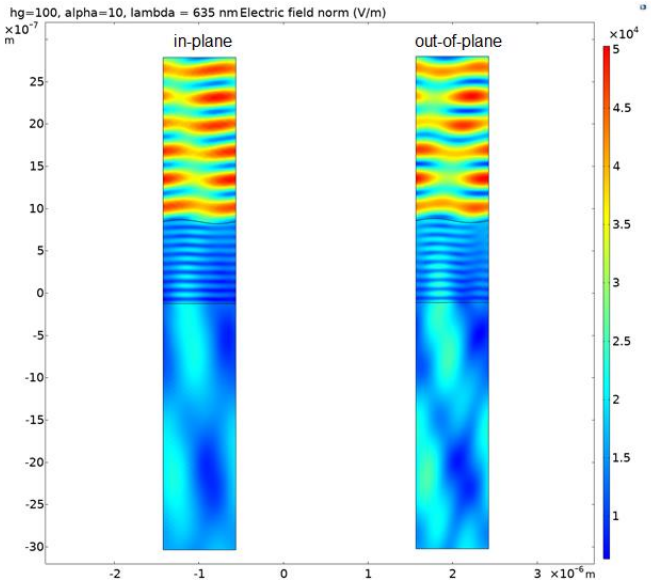

Figure 10. Spatial distribution of the electric field (electric field norm) for the red LED, $h = 100$ nm and $\alpha = 10$ deg.

Using the automatic diffraction order reflectance calculation, the results from this simulation can be again compared to the experiment and the analytical formula calculation. Similarly to the previous results, the 1st diffraction order reflectance is changing with the grating depth. The maximal values of the reflectance are lower than that for the green diode. The reflectance calculated using the COMSOL simulation is, in this case, closer to results obtained using analytical formula and also to experimental data (see figs. 11-12).

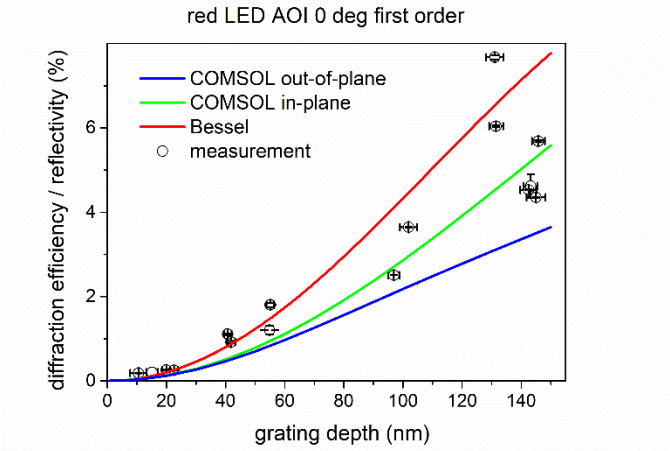

Figure 11. Comparison of the dependence of the 1st diffraction order reflectance / diffraction efficiency on grating depth for the red LED and $\alpha = 0$ deg obtained experimentally and theoretically.

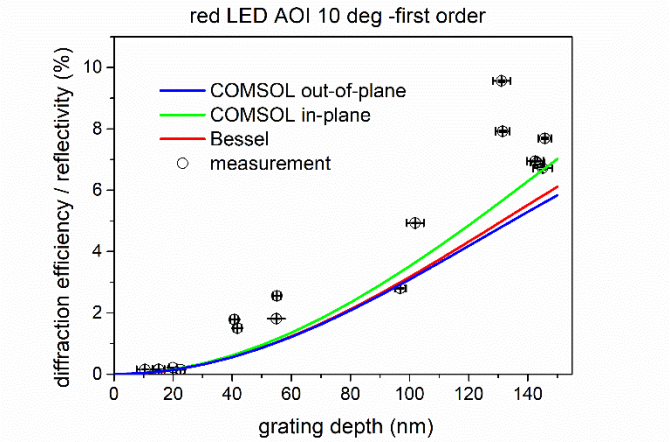

Figure 12. Comparison of the dependence of the minus 1st diffraction order reflectance / diffraction efficiency on grating depth for the red LED and $\alpha = 10$ deg obtained experimentally and theoretically.

Figure 13 shows remarkable difference between COMSOL calculation and results obtained using analytical formula. COMSOL is considering also the multiple reflection which are present due to the low absorption of the $As_{20}Se_{80}$ layer for the red light.

As it can be seen from Figure 13, although the experimental data are slightly lower than the expected results, they are definitely closer to COMSOL calculation results in case of red LED diode.

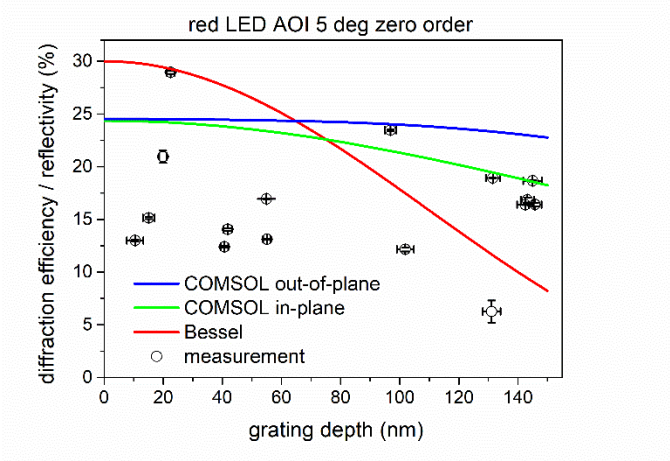

Figure 13. Comparison of the dependence of the zero diffraction order reflectance / diffraction efficiency on grating depth for the red LED and $\alpha = 5$ deg obtained experimentally and theoretically.

The transmittance calculated using the automatic diffraction order calculation (for [GH] in fig. 2) is about 45% (see fig. 14). The dependence of the 1st transmitted order on the grating depth can be used for experimental estimation of the grating depth with remark that values of transmittance are naturally lower than values of reflectance.

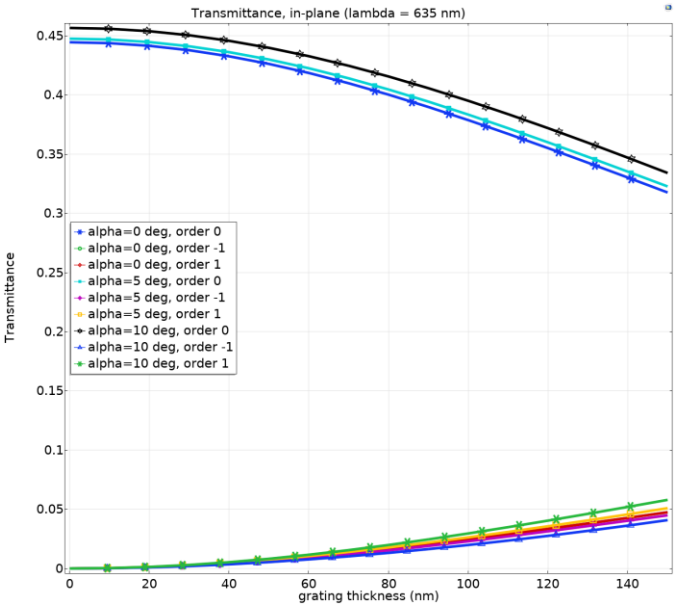

Figure 14. Dependence of the different diffraction order transmittance on grating depth for three angles of incidence.

Conclusions

COMSOL 5.5 with Wave Optics module has been used for the calculation of the electric field spatial distribution and reflectance of 1st, -1st and zero diffracted order for the diffraction grating with a sinusoidal profile. The parameters of the grating (grating period, thickness of the layer) were set according to values obtained experimentally. The optical

properties (refractive index and extinction coefficient) of the used materials were determined from spectroscopic ellipsometry measurements. The utilization of the procedure similar to Plasmonic wire grating model application, together with a parametric sweep, allows the comparison of the results calculated using two independent incident wave orientation (in-plane and out-of-plane) to the calculation using the analytical formula (without the sensitivity to the incident wave orientation) and the experimental data obtained using the custom-made diffraction efficiency measurement for our 16 diffraction gratings with different depth fabricated using hot-embossing. The results using the green LED diode obtained by COMSOL calculation are slightly higher in case of zero diffraction order (and consequently slightly lower for other diffraction orders) compared to analytical formula calculation and experimental results. Results for red LED diode obtained by COMSOL calculation are much closer to experimental data (especially for zero order) than the analytical formula.
Overall, a quite good agreement between experimental data and COMSOL calculation were obtained. This demonstrate that COMSOL can be used as an effective tool for diffraction efficiency modelling. Possible improvement of used model (influence of non-ideal sinusoidal profile, change of optical properties during hot-embossing, …) are planned to implement in order to explain difference obtained for green LED diode.

References

1. P. Hariharan, *Optical Holography: principles, techniques, and applications*, p. 47. Cambridge Studies in Modern Optics, second Edition (1996).
2. Ch. Palmer, E. Loewen, *Diffraction Grating Handbook*. Newport Corporation, USA (2014).
3. C. Newswangern: IS&T's 50th Annual Conference, p. 621, IS&T (1997).
(https://www.imaging.org/site/PDFS/Papers/1997/IST-0-4/175.pdf)

Acknowledgements

Authors appreciate financial support from grant LM2018103 from the Ministry of Education, Youth and Sports of the Czech Republic and European Regional Development Fund-Project "High-sensitive and low-density materials based on polymeric nanocomposites – NANOMAT"
(CZ.02.1.01/0.0/0.0/17_048/0007376).
Help from Linus Andersson (COMSOL Support) is appreciated.